Nonlinear Output Feedback Control of Underwater Vehicle Propellers using Advance Speed Feedback

Fossen, T.I.; Blanke, M.

Publication date:
1999

Document Version
Også kaldet Forlagets PDF

Nonlinear Output Feedback Control of Underwater Vehicle Propellers using Advance Speed Feedback

Thor I. Fossen*and Mogens Blanke†

To Appear in the EEE Journal of Oceanic Engineering in 2000.

Abstract

Accurate propeller shaft speed controllers can be designed by using nonlinear control theory and feedback from the advance speed of water going into the propeller. In this paper, an output feedback controller is derived, reconstructing the advance speed from vehicle speed measurements, using a three-state model of propeller shaft speed, forward (surge) speed of the vehicle and the advance speed. Lyapunov stability theory is used to prove that a nonlinear observer combined with an output feedback integral controller provide exponential stability. The output feedback controller compensates for variations in thrust due to time-variations in advance speed. This is a major problem when applying conventional vehicle-propeller control systems. The proposed controller is simulated for an underwater vehicle equipped with a single propeller. The simulations demonstrate that the advance speed can be estimated with good accuracy. In addition, the output feedback integral controller shows superior performance and robustness compared to a conventional RPM controller.

Keywords: Output feedback control, propeller shaft speed control, nonlinear control, underwater vehicles.

Nomenclature

u	Surge speed of vehicle (m/s)	D	Propeller diameter (m)
V_a	Advance speed (m/s)	T	Propeller thrust (N)
n	Propeller shaft speed (rps)	Q	Propeller torque (Nm)
ω_m	Profeller shaft speed (rad/s)	J_0	Advance ratio (-)
X_u	Linear damping coefficient in surge (kg/s)	K_T	Thrust coefficient (-)
$X_{u\|u\|}$	Quadratic damping coefficient in surge (kg/m)	K_Q	Torque coefficient (-)
$X_{\dot{u}}$	Added mass in surge (kg)	ρ	Density of water (kg/m^3)
t	Thrust deduction number (-)	ω_f	Natural frequency (rad/s)
w	Wake fraction number (-)	α_1, α_2	Thrust constants (-)
m_f	Mass of water in propeller control volume (kg)	β_1, β_2	Torque constants (-)
d_f	Linear damping coeff. for control volume (kg/s)	$T_{n\|n\|}$	Thrust coefficient (kgm)
d_0	Quadratic damping coeff. for control volume (kg/m)	$T_{\|n\|V_a}$	Thrust coefficient (kg)
K_n	Linear motor damping coefficient (kgm^2/s)	$Q_{n\|n\|}$	Torque coefficient (kgm^2)
$K_{n\|n\|}$	Nonlinear motor damping coefficient (kgm^2)	$Q_{\|n\|V_q}$	Torque coefficient (kgm)
J_m	Moment of inertia for DC-motor/propeller (kgm^2)	Q_0	Torque due to shaft speed (Nm)
V_m	DC motor armature voltage (Volt)	Q_1	Torque due to advance speed (Nm)
i_m	DC-motor armature current (A)	T_0	Thrust due to shaft speed (N)
τ	DC-motor control input (current, voltage or torque)	T_1	Thrust due to advance speed (N)
m	Mass of underwater vehicle (kg)	A_{surge}	Cross-sectional area in surge (m^2)
C_d	Drag coefficient (-)	A_{thruster}	Cross-sectional area of thruster (m^2)

*Department of Engineering Cybernetics, Norwegian University of Science and Technology, N-7491 Trondheim, Norway.
†Department of Automatic Control, Aalborg University, Fredrik Bajers Vej 7C, DK-9240 Aalborg, Denmark.

1 Introduction

Unmanned underwater vehicle (UUV) speed and position control systems are subject to an increased focus with respect to performance and safety. This is due to an increased number of commercially and militarily applications of UUVs. So far most focus has been directed towards the design of the outer-loop control system, that is speed and positioning control systems while the design of the propeller servo loops have received less attention. An overview of control methods for speed and positioning control of UUVs is found in Fossen [8] and references therein. This paper focuses on the design of a propeller shaft speed controller with feedback from estimated advance speed V_a. The motivation for the work is compensation of thruster losses due to variations in the magnitude of the propeller axial inlet flow.

In Yoerger et *al.* [28] a *one-state model* for propeller shaft speed n with thrust torque T as output is proposed. This model can be written:

$$\begin{aligned} 2\pi J_m \dot{n} + K_{n|n|} n\,|n| &= \tau && (1)\\ T &= T(n, V_a) && (2) \end{aligned}$$

where τ is the control input (shaft torque). For simplicity Yoerger et *al.* [28] assume that $V_a = 0$ when computing T. However, V_a can be measured by using a laser-Doppler velocimeter (LDV) system, a particle image velocimeter (PIV) system or an acoustic Doppler velocimeter system for instance. In this article a state observer for reconstruction of V_a will be designed, that is V_a is treated as an unmeasured state.

Healey et *al.* [10] have modified the models (1)–(2) to describe overshoots in thrust which are typical in experimental data. Based on the results of Cody [5] and McLean [16], Healey and co-workers propose a *two-state model*:

$$\begin{aligned} 2\pi J_m \dot{n} + K_n n &= \tau - Q(n, V_a) && (3)\\ m_f \dot{V}_a + d_f (V_a - u)\,|V_a - u| &= T(n, V_a) && (4)\\ T &= T(n, V_a) && (5) \end{aligned}$$

to include the dynamics of the advance speed V_a of the propeller and the forward speed u of the vehicle. This was done by modelling a control volume of water around the propeller as a *mass-damper* system. The mass-damper of the control volume interacts with the vehicle speed dynamics which also represents a *mass-damper* system.

Originally Healey et *al.* [10] considered a *voltage controlled motor*. However, as shown in Appendix A the model representation (3) can be used to describe:

- *Motor (armature) voltage control*
- *Motor (armature) current control*
- *Motor torque control*

The different DC-motor control strategies are obtained by choosing K_n and τ according to Table 2 in Appendix A. Experimental verifications of the *one-state* and *two-state* models are found in Whitcomb and Yoerger [26].

Based on the model of Healey et *al.* [10] and the results in Appendix A, we propose a *three-state* propeller shaft speed control model:

$$\begin{aligned} 2\pi J_m \dot{n} + K_n n &= \tau - Q(n, V_a) && (6)\\ m_f \dot{V}_a + d_0 (V_a - u) + d_f (V_a - u)\,|V_a - u| &= T(n, V_a) && (7)\\ (m - X_{\dot{u}})\dot{u} - X_u u - X_{u|u|} u\,|u| &= (1 - t) T(n, V_a) && (8)\\ T &= T(n, V_a) && (9) \end{aligned}$$

where damping in surge is modelled as the sum of *linear laminar skin friction,* $-X_u u$, (Faltinsen and Sortland [7]) and *nonlinear quadratic drag,* $-X_{u|u|} u\,|u|$, (Faltinsen [6]). Similarly, we have included linear damping, $d_0(V_a - u)$, and quadratic damping, $d_f (V_a - u)\,|V_a - u|$, in the axial flow model. Quadratic damping alone

would give an unrealistic response at low speeds since the damping at zero speed will be zero. The linear skin friction gives exponential convergence to zero at low speeds.

In the sequel, the unmeasured state V_a will be reconstructed by using a state observer. The objective is that propeller thrust $T(n, V_a)$ and torque $Q(n, V_a)$ can be computed for a time-varying V_a, resulting in a more accurate and robust control scheme than conventional shaft speed controllers where this effect is neglected.

1.1 Propeller Losses

When designing an UUV control system, commanded forces and moments must be realized by a propeller control system using a mapping from thrust demand to propeller revolution. This is a non-trivial task since a propeller in water suffers several phenomena that cause thrust losses. The primaries are:

Axial Water Inflow: Propeller losses caused by *axial water inflow*, that is the speed of the water going into the propeller. This is usually referred to as *advance speed*. The advance speed will in general differ from the speed of the vehicle. The dynamics of the propeller axial flow is usually neglected when designing the propeller shaft speed controller. This leads to thrust degradation since the computed thruster force is a function of both the propeller shaft speed and axial flow. The magnitude of the axial flow will strongly influence the thrust at high speed so it is crucial for the propeller performance.

Other effects that will reduce the propeller thrust were described in Sørensen et *al.* [23] and references therein. Some of these effects are:

Cross-Coupling Drag: Water inflow perpendicular to the propeller axis caused by current, vessel speed or jets from other thrusters. This will introduce a force in the direction of the inflow due to deflection of the propeller race.

Air Suction: For heavily loaded propellers ventilation (air suction) caused by decreasing pressure on the propeller blades may occur, especially when the submergence of the propeller becomes small due to the vessel's wave frequency motion.

In-and-out-of Water Effects: For extreme conditions with large vessel motions the *in-and-out-of water effects* will result in a sudden drop of thrust and torque following a hysteresis pattern.

Thruster Hull Interaction: Thrust reduction and change of thrust direction may occur due to thruster-hull interaction caused by frictional losses and pressure effects when the thruster race sweeps along the hull. The latter is the *Coanda effect* (Faltinsen [6], pp. 270–272).

Thruster-Thruster Interaction: Thruster-thruster interaction caused by influence from the propeller race from one thruster on neighboring thrusters may lead to significant thrust reduction.

1.2 Contributions

The main contributions of the paper are a globally exponentially stable (GES) nonlinear observer for estimation of advance speed using vessel speed and propeller revolution measurements (Theorem 1) and a nonlinear output feedback propeller shaft speed controller using feedback from the estimate of the advance speed (Theorem 2). The nonlinear shaft speed controller compensates for thrust losses due to time variations in advance speed and it is shown to provide superior thrust quality compared to conventional designs. The overall system is proven to be GES by applying Lyapunov stability theory. The proposed output feedback controller is a step towards the design of more sophisticated output feedback shaft speed propeller controllers minimizing some of the propeller losses listed in the previous section.

1.3 Outline

The paper is outlined as follows: Section 2 briefly reviews the theory of propeller thrust and torque modelling. Section 3 describes the modelling of the underwater vehicle dynamics and the axial flow dynamics of the propeller. In Section 4 a nonlinear observer for advance speed is proposed while Section 5 contains a

nonlinear output feedback controller for propeller shaft speed using the observer. Section 6 extends the results of Section 5 to integral control. Section 7 contains a case study with a UUV driven by a single propeller and Section 8 contains concluding remarks.

Figure 1: Schematic drawing of a propeller.

2 Propeller Thrust and Torque Modelling

For a fixed pitch propeller the shaft torque Q and force (thrust) T depend on the forward speed u of the vessel, the *advance speed* V_a (speed of the water going into the propeller) and the propeller rate n, see Figure 1. In addition, other dynamic effects due to *unsteady flows* will influence the propeller thrust and torque. According to Newman [20], Breslin and Andersen [3] and Carlton [4] the following *unsteady flow* effects are significant:

- *air suction*
- *cavitation*
- *in-and-out-of-water effects (Wagner's effect)*
- *wave influenced boundary layer effect*
- *Kuessner effect (gust)*

In this paper we are considering a deeply submerged vessel implying that the first four effects above can be neglected. The *Kuessner effect,* which is caused by a propeller in gust, will appear as a rapid oscillating thrust component. These fluctuations are usually small compared to the total thrust in a dynamical situation. In this paper, we will hence assume that this effect can be neglected as well. We can thus approximate the thrust and torque models with a *quasi-steady* representation. As a result, we limit our discussion to *quasi-steady* thrust and torque modelling while a dynamic model for shaft speed n, advance speed V_a, and surge velocity u will be presented

Unsteady modelling is, however, an important topic for future research since unsteady flow effects are significant in many practical situations in particular for surface vessels. A more detailed discussion on the accuracy of unsteady and quasi-steady modelling is found in Breslin and Andersen [3], pp. 374–386.

2.1 Quasi-Steady Thrust and Torque

Quasi-steady modelling of thrust and torque are usually done in terms of *lift* and *drag* curves which are transformed to thrust and torque by using the angle of incidence. This approach has been used by Yoerger et *al.* [28], Healey et *al.* [10] and Whitcomb and Yoerger [26] for instance.

The lift and drag are usually represented as *non-dimensional* thrust and torque coefficients computed from self-propulsion tests, see Fossen [8] or Lewis [13]. The *non-dimensional* thrust and torque coefficients K_T and K_Q are computed by measuring T, Q and n. Moreover:

$$K_T(J_0) = \frac{T}{\rho D^4 n\,|n|}, \quad K_Q(J_0) = \frac{Q}{\rho D^5 n\,|n|} \tag{10}$$

Here D is the propeller diameter, ρ is the water density and:

$$J_0 = \frac{V_a}{nD} \tag{11}$$

is the *advance ratio*. The numerical expressions for K_T and K_Q are found by *open water* tests, usually performed in a cavitation tunnel or a towing tank. These tests neglect the unsteady flow effects since steady-state values of T, Q and n are used.

The non-dimensional thrust and torque coefficients can also be described by the following parameters (Oosterveld and van Oossanen [22]):

$$K_T = f_1\left(J_0, \frac{P}{D}, \frac{A_E}{A_o}, Z\right) \tag{12}$$

$$K_Q = f_2\left(J_0, \frac{P}{D}, \frac{A_E}{A_o}, Z, R_n, \frac{t}{c}\right) \tag{13}$$

where P/D is the pitch ratio, A_E/A_0 is the expanded-area ratio, Z is the number of blades, R_n is the *Reynolds number*, t is the maximum thickness of the blade section, and c is the chord length of the blade section.

From (10) the thrust T and torque Q can be written

$$T = \rho D^4 K_T(J_0) n\,|n| \tag{14}$$

$$Q = \rho D^5 K_Q(J_0) n\,|n| \tag{15}$$

The open water propeller efficiency in undisturbed water is given as the ratio of the work done by the propeller in producing a thrust force divided by the work required to overcome the shaft torque according to:

$$\eta_o = \frac{V_a T}{2\pi n Q} = \frac{J_0}{2\pi} \cdot \frac{K_T}{K_Q} \tag{16}$$

K_T, K_Q, and η_o curves for different pitch ratios for a *Wageningen B-screw series* based on Table 5 in Oosterveld and van Oossanen [22], with $R_n = 2 \cdot 10^6$, $Z = 4$, $D = 3.1$ m, and $A_E/A_o = 0.52$ are shown in Figure 2.

For simplicity we will consider an underwater vehicle where K_T and K_Q show a linear behavior in J_0. Hence, we suggest to approximate:

$$K_T = \alpha_1 J_0 + \alpha_2 \tag{17}$$

$$K_Q = \beta_1 J_0 + \beta_2 \tag{18}$$

where α_i and β_i $(i = 1, 2)$ are four non-dimensional constants. It should be noted that nonlinear functions for K_T and K_Q can also be used. This is equivalent to the *lint theory* result, see Blanke [1]. Formulas (17)–(18) imply that the mathematical expressions for Q and T can be written as (Fossen [8], pp. 94–97):

$$T = T_{n|n|} n\,|n| - T_{|n|V_a}\,|n|\,V_a \tag{19}$$

$$Q = Q_{n|n|} n\,|n| - Q_{|n|V_a}\,|n|\,V_a \tag{20}$$

where

$$\begin{array}{ll} Q_{n|n|} = \rho D^5 \beta_2 & T_{n|n|} = \rho D^4 \alpha_2 \\ Q_{|n|V_a} = \rho D^4 \beta_1 & T_{|n|V_a} = \rho D^3 \alpha_1 \end{array} \tag{21}$$

are *positive* propeller coefficients given by the propeller characteristics. Notice that T and Q are defined for all n even though J_0 is undefined for $n = 0$. This is important since the observer-controller will be based on the expressions for T and Q.

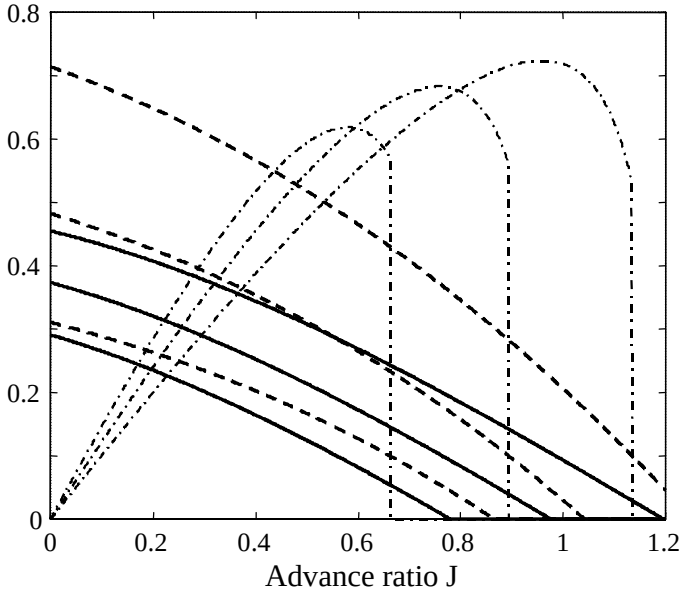

Figure 2: Open water K_T (solid), $10 \cdot K_Q$ (dash) and η_o (dash-dot) as a function of advance ratio J_0 for $P/D = 0.7$, 0.89 and 1.1. Reconstructed from data in [22].

3 Underwater Vehicle and Propeller Axial Flow Dynamics

Without loss of generality, we will consider an UUV moving in surge (x-direction) equipped with one single propeller aft of the hull (Figure 1). We also assume that the propeller is driven by a DC-motor, see Appendix A.

Let u (positive forwards) denote the forward speed of the underwater vehicle. The surge dynamics is assumed coupled to the *advance speed* of the propeller V_a (positive backwards) according to:

$$(m - X_{\dot{u}})\dot{u} - X_u u - X_{u|u|} u\,|u| = (1-t)T \tag{22}$$

$$m_f \dot{V}_a + d_0(V_a - u) + d_f(V_a - u)\,|V_a - u| = T \tag{23}$$

where $m_f > 0, d_0 > 0$ and $d_f > 0$. The vessel dynamics in surge (22) is modelled according to Fossen [8] where $m - X_{\dot{u}} > 0$ is the mass of the vessel including hydrodynamic added mass, $-X_u u - X_{u|u|} u\,|u| \geq 0$ is damping due to *linear skin friction* (Faltinsen and Sortland [7]) and *quadratic drag* (Lewis [13]), and $t > 0$ is the thrust deduction number (typically $0.05 - 0.2$) due to propeller-hull interactions.

The dynamics of the water (23) due to a control volume surrounding the inlet flow of the propeller is based on the work of Healey et *al.* [10], Cody [5] and McLean [16]. The only difference is that linear damping, $d_0(V_a - u)$, is added in addition to the quadratic term $d_f(V_a - u)\,|V_a - u|$ in order to produce more physical results at low speed, that is then $V_a - u$ is small. Hence, exponential convergence of V_a to u is guaranteed for $T = 0$. Notice that (23) represents a nonlinear *"hydrodynamic" mass-damper.*

For a vessel moving at positive cruise-speed in steady flow, u =constant and V_a =constant. The relationship between the steady-state speeds is defined as (Lewis [13]):

$$|V_a| = (1 - w)\,|u| \tag{24}$$

where $w > 0$ (typically $0.1 - 0.4$) is denoted as the *wake fraction number,* see also Sørensen et *al.* [23]. The static relationship (24) is not a good approximation for a dynamically positioned (DP) vehicle operating in the wave affected zone. Station-keeping implies that the propeller speed will oscillate about a slowly-varying mean depending on the wave, current and wind loads. This might lead to limit cycles if the propeller control system does not compensate for the dynamic effect due to the *"hydrodynamic" mass-damper* (23). Conventional propeller control systems do not include the effect of the advance speed V_a since this requires

that the propeller unit must be equipped with an additional sensor which can be quite expensive. In this paper, we will address the problem of nonlinear state estimation in order to reconstruct the state V_a from speed measurements u.

Determination of the Axial Flow Parameters $\mathbf{m}_f$ and $\mathbf{d}_f$

The axial flow damping coefficients can be related to the wake fraction number w in steady-state by considering the steady-state solutions of (22) and (23), that is:

$$-X_u u - X_{u|u|} u\,|u| = (1-t)\left[d_0(V_a - u) + d_f(V_a - u)\,|V_a - u|\right] \tag{25}$$

Substituting (24), yields:

$$(-X_u - (1-t)d_0 w)\,u + \left(-X_{u|u|} - (1-t)d_f w^2\right) u\,|u| = 0 \tag{26}$$

Solving this expression for d_0 and d_f under the assumption that $u \neq 0$, yields the following formulas:

$$d_0 = \frac{-X_u}{(1-t)w} > 0, \quad d_f = \frac{-X_{u|u|}}{(1-t)w^2} > 0 \tag{27}$$

since $t > 0$ and $w > 0$. The mass m_f of the control volume can be treated as a design parameter. A guideline could be to choose m_f according to Healey et *al.* [10]:

$$m_f = \rho A_{\text{thruster}} l\gamma > 0 \tag{28}$$

where ρ is the density of water, A_{thruster} is the cross-sectional area of the thruster, l is the length of the duct and $\gamma \geq 1.0$ is an empirically determined added mass coefficient. For conventional vehicles:

$$0 < m_f < m \tag{29}$$

Determination of the Hydrodynamic Coefficients $\mathbf{X}_{\dot{u}}$, $\mathbf{X}_u$ and $\mathbf{X}_{u|u|}$

The UUV model parameters can be found by using system identification (SI) methods, see Zhou and Blanke [29] for instance, hydrodynamic computation programs, semi-empirical methods or engineering judgement. For a slender body a first guess could be (Fossen [8]):

$$-X_{\dot{u}} = (0.05 - 0.10) \cdot m \tag{30}$$

The damping coefficients can be found by as:

$$-X_u = \frac{m - X_{\dot{u}}}{T_{\text{surge}}}, \qquad -X_{u|u|} = \frac{1}{2}\rho C_d A_{\text{surge}} \tag{31}$$

where $T_{surge} > 0$ is a design parameter (time constant in surge), C_d is the drag coefficient and A_{surge} is the cross-sectional area in surge as defined by *Morrison's equation,* see Lewis [13]. Alternatively, $-X_u$ and $-X_{u|u|}$ can be found by performing a *free decay test* (Faltinsen [6]).

3.1 Resulting Model for Vehicle Speed and Propeller Axial Flow Dynamics

Equations (22)–(23) and (19) can be combined to give:

$$\begin{bmatrix} m - X_{\dot{u}} & 0 \\ 0 & m_f \end{bmatrix} \begin{bmatrix} \dot{u} \\ \dot{V}_a \end{bmatrix} + \begin{bmatrix} -X_u - X_{u|u|}\,|u| & 0 \\ -d_0 - d_f\,|V_a - u| & d_0 + d_f\,|V_a - u| \end{bmatrix} \begin{bmatrix} u \\ V_a \end{bmatrix} + |n| \begin{bmatrix} 0 & (1-t)T_{|n|V_a} \\ 0 & T_{|n|V_a} \end{bmatrix} \begin{bmatrix} u \\ V_a \end{bmatrix} = \begin{bmatrix} (1-t)T_{n|n|}\,n\,|n| \\ T_{n|n|}\,n\,|n| \end{bmatrix} \tag{32}$$

The measurement equation is:

$$y = \begin{bmatrix} 1 & 0 \end{bmatrix} \begin{bmatrix} u \\ V_a \end{bmatrix} \tag{33}$$

This can be written in state-space form according to:

$$\begin{aligned} \mathcal{H}\dot{\mathbf{x}} + \mathcal{D}_0\mathbf{x} + \mathcal{D}_1(\mathbf{x},y)\mathbf{x} + |n|\,\mathcal{E}\mathbf{x} &= \mathbf{f}(n) && (34)\\ y &= \mathbf{h}^T\mathbf{x} && (35) \end{aligned}$$

where $\mathbf{x} = [u, V_a]^T$, $y = u$ and

$$\begin{aligned} \mathcal{H} &= \begin{bmatrix} m - X_{\dot{u}} & 0 \\ 0 & m_f \end{bmatrix} && (36)\\ \mathcal{D}_0 &= \begin{bmatrix} -X_u & 0 \\ -d_0 & d_0 \end{bmatrix} && (37)\\ \mathcal{D}_1(\mathbf{x},y) &= \begin{bmatrix} -X_{u|u|}\,|u| & 0 \\ -d_f\,|V_a - y| & d_f\,|V_a - y| \end{bmatrix} && (38)\\ \mathcal{E} &= \begin{bmatrix} 0 & (1-t)T_{|n|V_a} \\ 0 & T_{|n|V_a} \end{bmatrix} && (39)\\ \mathbf{f}(n) &= \begin{bmatrix} (1-t)T_{n|n|}\,n\,|n| \\ T_{n|n|}\,n\,|n| \end{bmatrix} && (40)\\ \mathbf{h}^T &= \begin{bmatrix} 1 & 0 \end{bmatrix} && (41) \end{aligned}$$

4 Nonlinear Observer for Propeller Axial Flow

A nonlinear observer for shaft speed estimation and fault detection has been proposed by Blanke, Izadi-Zamanabadi and Lootsma [2] under the assumption that the effect of the propeller axial inlet flow V_a can be neglected. They have proven semi-global asymptotic and (local) exponential stability for the case with quadratic damping.

Nonlinear observers for underwater vehicles can also be designed by using contraction analysis as described by Lohmiller [17], pp. 38–42, Lohmiller and Slotine [18], [19]. This is based on the method of Lewis [14] where it is shown that the *Riemann* metric can be used as a tool for contraction analysis of non-autonomous nonlinear systems. Furthermore, combination properties of contracting systems can be exploited to design globally convergent observer-controllers for shaft speed output feedback control which is attractive due to design simplicity and good convergence properties.

The focus of this paper is Lyapunov-based output feedback control and global exponential stability properties which are important from a robust performance point of view. This gives a different observer structure than the one obtained from contraction analysis. For a more detailed discussion on nonlinear observer-controller design see Nijmeijer and Fossen [21] and references therein.

4.1 Observer Equations

In this section, we will derive a nonlinear state observer for the unmeasured state V_a and use this result as a basis for the nonlinear controller. The main motivation for this is that the control law should exploit V_a in the design in order to reduce propeller losses. This is done by choosing the following observer structure copying the dynamics (34)–(35):

$$\begin{aligned} \mathcal{H}\dot{\hat{\mathbf{x}}} + \mathcal{D}_0\hat{\mathbf{x}} + \mathcal{D}_1(\hat{\mathbf{x}},y)\hat{\mathbf{x}} + |n|\,\mathcal{E}\hat{\mathbf{x}} &= \mathbf{f}(n) + \mathbf{k}(n)\tilde{y} && (42)\\ \hat{y} &= \mathbf{h}^T\hat{\mathbf{x}} && (43) \end{aligned}$$

where $\tilde{y} = y - \hat{y}$ and an intelligent guess for the observer gain vector is:

$$\mathbf{k}(n) = \begin{bmatrix} K_{10} \\ K_{20} \end{bmatrix} + |n| \begin{bmatrix} K_{11} \\ K_{21} \end{bmatrix} \tag{44}$$

The error dynamics corresponding to $\tilde{\mathbf{x}} = \mathbf{x} - \hat{\mathbf{x}}$ becomes:

$$\mathcal{H}\dot{\tilde{\mathbf{x}}} = -\left(\mathcal{D}_0 + |n|\,\mathcal{E} + \mathbf{k}(n)\mathbf{h}^T\right)\tilde{\mathbf{x}} - \boldsymbol{\delta}(\mathbf{x},\hat{\mathbf{x}},y) \tag{45}$$

where the nonlinear estimation error term $\boldsymbol{\delta}(\mathbf{x},\hat{\mathbf{x}},y)$ is:

$$\boldsymbol{\delta}(\mathbf{x},\hat{\mathbf{x}},y) = \mathcal{D}_1(\mathbf{x},y)\mathbf{x} - \mathcal{D}_1(\hat{\mathbf{x}},y)\hat{\mathbf{x}} = \begin{bmatrix} (-X_{u|u|})\,|u|\,u - (-X_{u|u|})\,|\hat{u}|\,\hat{u} \\ d_f\,|V_a - y|\,(V_a - y) - d_f\left|\hat{V}_a - y\right|(\hat{V}_a - y) \end{bmatrix} \tag{46}$$

Defining:

$$\mathcal{F} = \begin{bmatrix} -X_u + K_{10} & 0 \\ -d_0 + K_{20} & d_0 \end{bmatrix}, \quad \mathcal{G} = \begin{bmatrix} K_{11} & (1-t)T_{|n|V_a} \\ K_{21} & T_{|n|V_a} \end{bmatrix} \tag{47}$$

implies that (45) can be written:

$$\mathcal{H}\dot{\tilde{\mathbf{x}}} = -\mathcal{F}\tilde{\mathbf{x}} - |n|\,\mathcal{G}\tilde{\mathbf{x}} - \boldsymbol{\delta}(\mathbf{x},\hat{\mathbf{x}},y) \tag{48}$$

We will now show how the elements in the observer gain vector $\mathbf{k}(n)$ can be chosen such that the equilibrium point $\tilde{\mathbf{x}} = \mathbf{0}$ is GES.

4.2 Lyapunov Analysis

Consider the Lyapunov function candidate:

$$V_{\text{obs}}(\tilde{\mathbf{x}},t) = \tilde{\mathbf{x}}^T\mathcal{H}\tilde{\mathbf{x}} \tag{49}$$

$$\dot{V}_{\text{obs}}(\tilde{\mathbf{x}},t) = -\tilde{\mathbf{x}}^T\left(\mathcal{F}+\mathcal{F}^T\right)\tilde{\mathbf{x}} - |n|\,\tilde{\mathbf{x}}^T\left(\mathcal{G}+\mathcal{G}^T\right)\tilde{\mathbf{x}} - 2\tilde{\mathbf{x}}^T\boldsymbol{\delta}(\mathbf{x},\hat{\mathbf{x}},y) \tag{50}$$

where the design goal is to choose K_{10}, K_{20}, K_{11} and K_{21} such that $\dot{V}_{\text{obs}} < 0$ for all $\tilde{\mathbf{x}} \neq \mathbf{0}$.

For a *nondecreasing function* $f(x)$ it can be shown that:

$$(x - \hat{x})\,(f(x) - f(\hat{x})) \geq 0 \tag{51}$$

From (51) it is seen that the nonlinear coupling term $\tilde{\mathbf{x}}^T\boldsymbol{\delta}$ in $\dot{V}_{\text{obs}}$ satisfies:

$$\begin{aligned} \tilde{\mathbf{x}}^T\boldsymbol{\delta}(\mathbf{x},\hat{\mathbf{x}},y) &= (u - \hat{u})\,\delta_1 + (V_a - \hat{V}_a)\delta_2 \\ &= (u - \hat{u})\,(-X_{u|u|})\,(|u|\,u - |\hat{u}|\,\hat{u}) \\ &\quad + \left((V_a - y) - (\hat{V}_a - y)\right) d_f\left(|V_a - y|\,(V_a - y) - \left|\hat{V}_a - y\right|(\hat{V}_a - y)\right) \\ &\geq 0 \end{aligned} \tag{52}$$

since $-X_{u|u|} > 0$ and $d_f > 0$. This is due to the fact that dissipative damping terms like quadratic drag, $u\,|u|$, and also higher order terms in $u\,|u|^n$ $(n = 1, 2, 3...)$ are all *nondecreasing*. Therefore:

$$\dot{V}_{\text{obs}}(\tilde{\mathbf{x}},t) \leq -\tilde{\mathbf{x}}^T\left(\mathcal{F}+\mathcal{F}^T\right)\tilde{\mathbf{x}} - |n|\,\tilde{\mathbf{x}}^T\left(\mathcal{G}+\mathcal{G}^T\right)\tilde{\mathbf{x}} \tag{53}$$

Next we notice that the last term in (53) is zero if $n = 0$. For non-zero values of n we therefore require that:

$$\mathcal{G}+\mathcal{G}^T = \begin{bmatrix} 2K_{11} & (1-t)T_{|n|V_a} + K_{21} \\ (1-t)T_{|n|V_a} + K_{21} & 2T_{|n|V_a} \end{bmatrix} > 0 \tag{54}$$

which is easy to satisfy since K_{11} and K_{21} can be chosen such that:

$$\begin{aligned} K_{11} &> 0 && (55)\\ 4K_{11}T_{|n|V_a} &> \left((1-t)T_{|n|V_a}+K_{21}\right)^2 && (56)\end{aligned}$$

Hence,

$$\dot{V}_{\text{obs}}(\tilde{\mathbf{x}},t) \leq -\tilde{\mathbf{x}}^T\left(\mathcal{F}+\mathcal{F}^T\right)\tilde{\mathbf{x}} \quad (57)$$

We will now show that the remaining two gains K_{10} and K_{20} can be chosen such that:

$$\begin{aligned} \dot{V}_{\text{obs}}(\tilde{\mathbf{x}},t) &\leq -\tilde{\mathbf{x}}^T\left(\mathcal{F}+\mathcal{F}^T\right)\tilde{\mathbf{x}}\\ &\leq -q_1\tilde{u}^2 - q_2\tilde{V}_a^2\\ &< 0, \forall \tilde{u}\neq 0, V_a \neq 0 && (58)\end{aligned}$$

where $q_1 > 0$ and $q_2 > 0$. In order to prove this we will make use of the following lemma:

Lemma 1 (Negative Quadratic Form) *The quadratic form:*

$$\dot{V} = -\mathbf{x}^T\mathbf{P}\mathbf{x} \quad (59)$$

with $\mathbf{P} = \{p_{ij}\}$ *is bounded by*

$$\dot{V} \leq -q_1x_1^2 - q_2x_2^2 \quad (60)$$

where

$$\begin{aligned} q_1 &= p_{11}-\beta > 0 && (61)\\ q_2 &= p_{22} - \frac{(p_{12}+p_{21})^2}{4\beta} > 0, \qquad \beta > 0 && (62)\end{aligned}$$

if:

$$\begin{aligned} p_{11} &> \beta > 0 && (63)\\ p_{22} &> \frac{(p_{12}+p_{21})^2}{4\beta} > 0 && (64)\end{aligned}$$

Proof. Expanding $\dot{V}$, yields:

$$\begin{aligned} \dot{V} &= -p_{11}x_1^2 - (p_{12}+p_{21})x_1x_2 - p_{22}x_2^2\\ &= -(p_{11}-\beta)x_1^2 - \left(\sqrt{\beta}x_1 + \frac{(p_{12}+p_{21})}{2\sqrt{\beta}}x_2\right)^2 - \left(p_{22} - \frac{(p_{12}+p_{21})^2}{4\beta}\right)x_2^2\\ &\leq -\underbrace{(p_{11}-\beta)}_{q_1}x_1^2 - \underbrace{\left(p_{22} - \frac{(p_{12}+p_{21})^2}{4\beta}\right)}_{q_2}x_2^2 && (65)\end{aligned}$$

From this it is seen that (63)–(64) implies that $q_1 > 0$ and $q_2 > 0$ and therefore that $\dot{V} < 0$ for all $x_1 \neq 0$ and $x_2 \neq 0$. ■

Theorem 1 (GES Nonlinear Observer Error Dynamics) *The equilibrium point* $\tilde{\mathbf{x}} = \mathbf{0}$ *of the observer error dynamics (48) is GES if* K_{11} *and* K_{21} *are chosen such that* $\mathcal{G}+\mathcal{G}^T > 0$*, that is:*

$$\begin{aligned} K_{11} &> 0 && (66)\\ 4K_{11}T_{|n|V_a} &> \left((1-t)T_{|n|V_a}+K_{21}\right)^2 && (67)\end{aligned}$$

while K_{10} *and* K_{20} *must satisfy:*

$$\begin{aligned} 2d_0\beta &> (-d_0+K_{20})^2 && (68)\\ K_{10}-X_u &> \frac{1}{2}\beta && (69)\end{aligned}$$

where $\beta > 0$.

Proof. Let

$$\mathbf{P} = \mathcal{F} + \mathcal{F}^T = \begin{bmatrix} 2(-X_u + K_{10}) & -d_0 + K_{20} \\ -d_0 + K_{20} & 2d_0 \end{bmatrix} \tag{70}$$

in Lemma 1. Hence,

$$p_{11} = 2(-X_u + K_{10}) > \beta > 0 \tag{71}$$

$$p_{22} = 2d_0 > \frac{(2(-d_0 + K_{20}))^2}{4\beta} > 0 \tag{72}$$

directly implies (68)–(69). It then follows that $\dot{V} \leq -q_1 x_1^2 - q_2 x_2^2$ with $q_1 > 0$ and $q_2 > 0$. Hence, it follows from Lyapunov stability theory that the equilibrium point $\tilde{\mathbf{x}} = \mathbf{0}$ is GES if $\beta > 0$. ■

It should be noted that we have not considered bias state estimation when designing the observer. In a practical implementation it might be necessary to augment a constant bias term to the dynamic model in order to improve robustness to unmodelled dynamics and parametric uncertainties. Bias state estimation for ships have been discussed by Fossen and Strand [9] and, Zhou and Blanke [29].

5 Definition of the Control Problem

The control objective is to design a propeller shaft speed controller tracking the desired propeller revolution n_d (inner loop controller) by compensating the axial flow dynamics V_a. The desired propeller rate of revolution is generated by the UUV speed controller where u_d denotes the desired vessel speed (outer loop controller).

The dynamics of the two control loops can be summarized according to:

UUV Speed Control Loop

The surge dynamics of the UUV is:

$$\dot{x} = u \tag{73}$$

$$(m - X_{\dot{u}})\dot{u} - X_u u - X_{u|u|} u\,|u| = (1 - t)T \tag{74}$$

where T is the control input (force) generated by a speed controller

$$T = T(\dot{u}_d, u_d, u) \tag{75}$$

designed such that $u \to u_d$.

Propeller Shaft Speed Control Loop

The desired shaft speed is found from (19) as:

$$n_d' = \frac{T_{|n|V_a} + \text{sign}(T_d)\sqrt{\left|T_{|n|V_a}^2 V_a^2 + 4T_{|n|n} T_d\right|}}{2T_{|n|n}}$$

$$= \omega(T_d, V_a) \tag{76}$$

$$\ddot{n}_d + 2\omega_f \dot{n}_d + \omega_f^2 n_d = \omega_f^2 n_d', \quad \omega_f > 0 \tag{77}$$

where T_d is the desired thrust and (77) is a 2nd-order low-pass filter with natural frequency ω_f used to generate two smooth reference signal n_d and $\dot{n}_d$. These signals are again used as reference for the propeller controller:

$$\tau = \tau(\dot{n}_d, n_d, n, V_a) \tag{78}$$

corresponding to the *two-state* actuator dynamics:

$$\dot{n} = \phi_1(n, Q(n, V_a), \tau) \tag{79}$$
$$\dot{V}_a = \phi_2(n, V_a, u) \tag{80}$$
$$T = T(n, V_a) \tag{81}$$

This model is similar to the model of Healey et *al.* [10] except for that we have included the effect of the forward speed u in the expression for the V_a-dynamics. The two control loops are shown in Figure 3 indicating how a nonlinear shaft speed propeller controller together with a conventional UUV speed controller should exploit the estimate of the propeller axial flow $\hat{V}_a$. It is also seen that this is a nonlinear output feedback control problem. One solution to this control problem is to apply *observer backstepping* (Krstic et *al.* [12]). This is the topic for the next section.

Experiments with different RPM control strategies and position control of underwater vehicles are reported in Tsukamoto et *al.* [24] and Whitcomb and Yoerger [27].

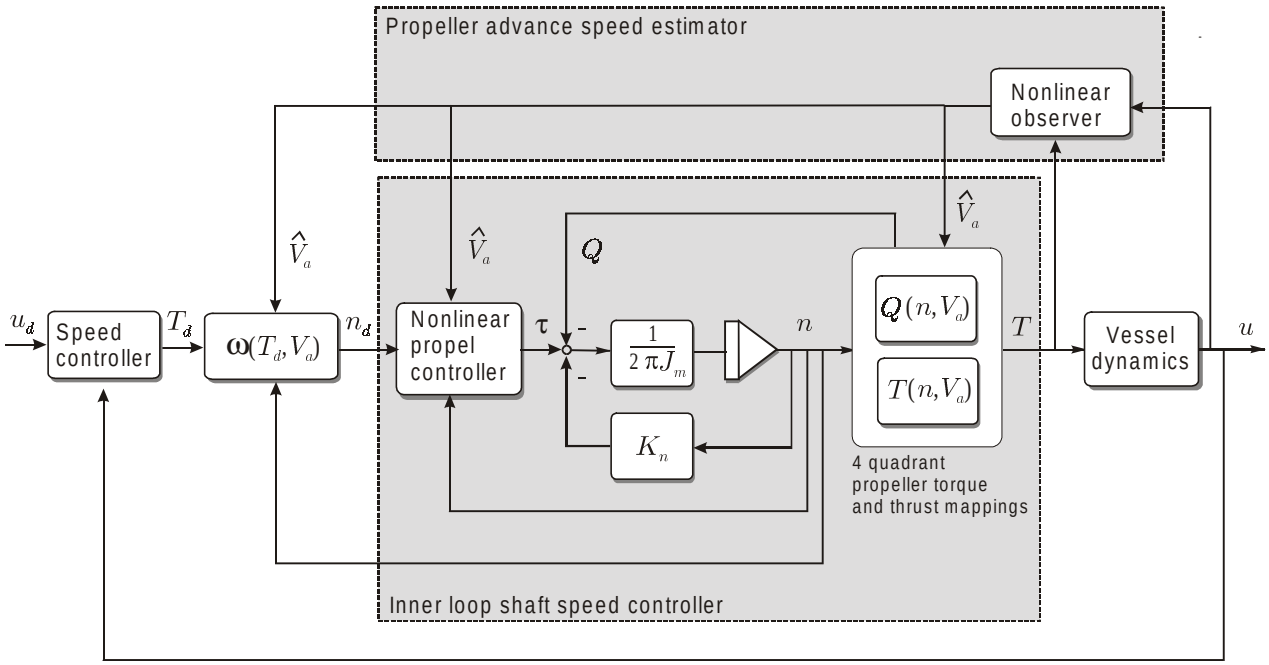

Figure 3: Block diagram showing the two control loops.

6 Nonlinear Output Feedback Control Design

In this section we will design a nonlinear output feedback propeller controller using only surge speed measurements u and propeller revolution measurements n. The advance speed of the water V_a will be estimated by the state estimator (42)–(43) which was proven to be GES (Theorem 1). The design goal is to render the closed-loop error dynamics of the observer-controller GES.

6.1 Nonlinear Model for Propeller Shaft Speed Control

Consider the unified DC-motor model (Appendix A):

$$2\pi J_m \dot{n} + K_n n = \tau - Q(n, V_a) \tag{82}$$

which can be used to describe motor *voltage, current* and *torque* controlled propellers. Substituting the expression for Q given by (20) into (82), yields the 3rd-order model:

$$\begin{aligned} 2\pi J_m \dot{n} &= -(K_n + Q_{n|n|}\,|n|)n + Q_{|n|V_a}\,|n|\,V_a + \tau && (83)\\ \mathcal{H}\dot{\mathbf{x}} + \mathcal{D}_0\mathbf{x} + \mathcal{D}_1(\mathbf{x},y)\mathbf{x} + |n|\,\mathcal{E}\mathbf{x} &= \mathbf{f}(n) && (84)\\ y &= \mathbf{h}^T\mathbf{x} && (85) \end{aligned}$$

6.2 Lyapunov Analysis

The observer (42) is used to generate an estimate $\hat{V}_a$ of V_a. Consider the control Lyapunov function candidate:

$$\begin{aligned} V &= V_{\text{obs}} + \pi J_m \tilde{n}^2 && (86)\\ \dot{V} &\leq -q_1\tilde{u}^2 - q_2\tilde{V}_a^2 + 2\pi J_m \tilde{n}\dot{\tilde{n}} && (87) \end{aligned}$$

where $\tilde{n} = n - n_d$ is the tracking error. Substituting (83) into (87), yields:

$$\dot{V} \leq -q_1\tilde{u}^2 - q_2\tilde{V}_a^2 + \tilde{n}(\tau - 2\pi J_m \dot{n}_d - (K_n + Q_{n|n|}\,|n|)n + Q_{|n|V_a}\,|n|\,V_a) \quad (88)$$

The expression for $\dot{V}$ suggests that the control law τ should be chosen to include three parts: (1) a nonlinear P-controller, $-(K_{p0} + K_{p1}n^2)\tilde{n}$, (2) a nonlinear feedforward term based on the measured propeller revolution n and the desired propeller revolution n_d, and (3) a nonlinear cross-term, $-Q_{|n|V_a}\,|n|\,\hat{V}_a$, compensating for the axial flow into the propeller. This is the main result of the paper.

Theorem 2 (GES Nonlinear Observer-Controller Error Dynamics) *Consider the nonlinear shaft speed controller:*

$$\tau = \underbrace{-(K_{p0} + K_{p1}n^2)\tilde{n}}_{P\text{-}control} + \underbrace{2\pi J_m \dot{n}_d + (K_n + Q_{n|n|}\,|n|)n_d}_{Reference\ Feed\ Forward} - \underbrace{Q_{|n|V_a}\,|n|\,\hat{V}_a}_{Axial\ Flow\ Compensator} \quad (89)$$

with

$$K_{p0} > 0, \quad K_{p1} > \frac{1}{4}(Q_{|n|V_a})^2 > 0 \quad (90)$$

Let the estimate $\hat{V}_a$ be generated by using the nonlinear observer (42)–(43) with $q_2 > 1$ in Theorem 1 implying that K_{20} must satisfy the stronger requirement $2d_0\beta > 1 + (-d_0 + K_{20})^2$. Hence, the equilibrium point $(\tilde{u}, \tilde{V}_a, \tilde{n}) = (0,0,0)$ of the observer-controller error dynamics:

$$\mathcal{M}\dot{\tilde{\boldsymbol{\nu}}} + \mathcal{D}(\boldsymbol{\nu})\tilde{\boldsymbol{\nu}} + \mathrm{d}(\boldsymbol{\nu}, \tilde{\boldsymbol{\nu}}, y) = \mathbf{0} \quad (91)$$

where $\mathbf{v} = [u, V_a, n]^T$ and:

$$\begin{aligned} \mathcal{M} &= \begin{bmatrix} m - X_{\dot{u}} & 0 & 0 \\ 0 & m_f & 0 \\ 0 & 0 & 2\pi J_m \end{bmatrix} && (92)\\ \mathcal{D}(\boldsymbol{\nu}) &= \begin{bmatrix} -K_{10} - K_{11}\,|n| - X_u & (1-t)T_{|n|V_a}\,|n| & 0 \\ -K_{20} - K_{21}\,|n| - d_0 & d_0 + T_{|n|V_a}\,|n| & 0 \\ 0 & -Q_{|n|V_a}\,|n| & K_{p0} + K_{p1}n^2 + K_n + Q_{n|n|}\,|n| \end{bmatrix} && (93)\\ \mathrm{d}(\boldsymbol{\nu}, \tilde{\boldsymbol{\nu}}, y) &= \begin{bmatrix} (-X_{u|u|})u\,|u| - (-X_{u|u|})\,|u - \tilde{u}|\,(u - \tilde{u}) \\ d_f(V_a - y)\,|V_a - y| - d_f(V_a - \tilde{V}_a - y)\left|V_a - \tilde{V}_a - y\right| \\ 0 \end{bmatrix} && (94) \end{aligned}$$

is GES.

Proof. Substituting (89) into (88), yields:

$$\dot{V} \leq -q_1\tilde{u}^2 - q_2\tilde{V}_a^2 + Q_{|n|V_a}\,|n|\,\tilde{V}_a\tilde{n} - (K_{p0} + K_{p1}n^2 + K_n + Q_{n|n|}\,|n|)\tilde{n}^2 \tag{95}$$

Using the fact that

$$-\left(\frac{1}{2}Q_{|n|V_a}\,|n|\,\tilde{n} - \tilde{V}_a\right)^2 = -\frac{1}{4}Q_{|n|V_a}^2 n^2\tilde{n}^2 + Q_{|n|V_a}\,|n|\,\tilde{n}\tilde{V}_a - \tilde{V}_a^2 \tag{96}$$

Hence, the cross term in (95) can be replaced by:

$$Q_{|n|V_a}\,|n|\,\tilde{n}\tilde{V}_a = -\left(\frac{1}{2}Q_{|n|V_a}\,|n|\,\tilde{n} - \tilde{V}_a\right)^2 + \frac{1}{4}Q_{|n|V_a}^2 n^2\tilde{n}^2 + \tilde{V}_a^2 \tag{97}$$

implying that:

$$\begin{aligned}
\dot{V} \;&\leq\; -q_1\tilde{u}^2 - (q_2 - 1)\,\tilde{V}_a^2 - \left(K_{p1} - \frac{1}{4}(Q_{|n|V_a})^2\right) n^2\tilde{n}^2 \\
&\quad - \left(\frac{1}{2}Q_{|n|V_a}\,|n|\,\tilde{n} - \tilde{V}_a\right)^2 - \left(K_{po} + K_n + Q_{n|n|}\,|n|\right)^2\tilde{n}^2 \\
&<\; 0, \forall\tilde{u} \neq 0, \tilde{V}_a \neq 0, \tilde{n} \neq 0
\end{aligned} \tag{98}$$

Hence, according to Lyapunov stability theory the equilibrium point $(\tilde{u}, \tilde{V}_a, \tilde{n}) = (0, 0, 0)$ of the observer-controller error dynamics (91) is GES if $q_1 > 0, q_2 > 1, K_{p0} > 0$ and $K_{p1} > (1/4)(Q_{|n|V_a})^2$. ■

7 Extensions to Integral Control

When implementing the shaft speed propeller controller, it is important to include integral action in order to compensate for non-zero slowly-varying disturbances and unmodelled dynamics. This can be done by augmenting a constant bias term b to (82) according to:

$$2\pi J_m\dot{n} = -K_n n + \tau - Q(n, V_a) + b \tag{99}$$

$$\dot{b} = 0 \tag{100}$$

Choosing the nonlinear control law of PI-type with reference feedforward and axial flow compensation, that is:

$$\tau = \underbrace{-(K_{p0} + K_{p1}n^2)\tilde{n} - \hat{b}}_{\text{PI-control}} + \underbrace{2\pi J_m\dot{n}_d + (K_n + Q_{n|n|}\,|n|)n_d}_{\text{Reference Feed Forward}} - \underbrace{Q_{|n|V_a}\,|n|\,\hat{V}_a}_{\text{Axial Flow Compensator}} \tag{101}$$

$$\dot{\hat{b}} = K_i\tilde{n}, \quad K_i > 0 \tag{102}$$

implies that (91) takes the form:

$$\dot{\mathbf{x}}_1 = \mathbf{h}(\mathbf{x}_1, t) + \mathbf{g}x_2 + \mathbf{d} \tag{103}$$

$$\dot{x}_2 = -K_i\mathbf{g}^T\mathbf{x}_1 \tag{104}$$

with $\mathbf{x}_1 = \tilde{\mathbf{v}} \in \Re^3$, $x_2 = \hat{b} - b \in \Re$ and

$$\mathbf{h}(\mathbf{x}_1, t) = -\mathcal{M}^{-1}\mathcal{D}(\mathbf{x}_1 + \boldsymbol{\nu}_d(t))\mathbf{x}_1 \tag{105}$$

$$\mathbf{g} = \mathcal{M}^{-1}\begin{bmatrix} 0 \\ 0 \\ -1 \end{bmatrix} = \begin{bmatrix} 0 \\ 0 \\ -\frac{1}{2\pi J_m} \end{bmatrix} \tag{106}$$

$$\mathbf{d} = -\mathcal{M}^{-1}d \tag{107}$$

where we have used that $\boldsymbol{\nu} = \mathbf{x}_1 + \boldsymbol{\nu}_d$. The error dynamics (103)–(104) is a *nonlinear non-autonomous* system complicating the Lyapunov stability analysis since $\dot{V} \leq 0$ is only *negative semi-definite*. Hence, *LaSalle-Krasovskii's theorem* for invariant manifolds cannot be used (Khalil [11]) to prove uniformly globally asymptotic stability (UGAS). However, UGAS and uniformly locally exponentially stability (ULES) of the equilibrium point $(\mathbf{x}_1^T, x_2) = (0, 0, 0, 0)$ of the error dynamics (103)–(104) can be proven by applying the main result of Loria, Fossen and Teel [15] which is a theorem for *"backstepping with integral action"*. The interested reader is recommended to consult [15] for the technicalities regarding the proof.

8 Case Study

In the simulation study the following two controllers were compared:

- *Nonlinear output feedback integral control* where the nonlinear observer (Theorem 1) was simulated by using the following gains:

$$\begin{aligned} \beta &= -10X_u \\ K_{10} &= 1.0 \cdot (m - X_{\dot{u}}), \qquad K_{20} = 0.1 \cdot m_f \\ K_{11} &= 0.005 \cdot (m - X_{\dot{u}}), \quad K_{21} = -30 \end{aligned}$$

  while the control gains in (Theorem 2) were chosen as:

$$K_{p0} = 1.0, \quad K_{p1} = \frac{1}{4}(Q_{|n|V_a})^2, \quad K_i = 1.0$$

  When simulating the observer-controller it is noticed that performance improvements can be obtained by reducing the controller gains in particular if the measurements are noisy. It is well known that the gain requirements imposed by the Lyapunov analysis are rather conservative. Moreover, the closed-loop system can be exponential stable for much smaller gains than those given by Theorem 2. In fact, we noticed that the performance was significantly improved when K_{p1} was reduced by a factor of 10 and this did not affect the stability of the closed-loop system.

- *Conventional shaft speed control of PI-type:*

$$\tau = -K_p(n - n_d) - K_i \int_0^t (n - n_d) d\tau \tag{108}$$

  with

$$K_p = 10.0, \quad K_i = 1.0$$

For both controllers the torque controlled representation of the DC-motor (125) was used.

8.1 Model Parameters

The model parameters are given in Table 1. The propeller characteristics were taken from an experiment with a full-scale propeller, see Figure 4.

Least-squares curve fitting of K_T and K_Q gave the following results (straight lines in Figure 4):

$$K_T = -0.9435\ J_0 + 0.4243 \tag{109}$$

$$K_Q = -0.1212\ J_0 + 0.0626 \tag{110}$$

Even though this over-all linear approximation is crude, in particular for reverse conditions ($J_0 < 0$), the observer observer is able to cope with the model inaccuracies and give a useful estimate of V_a.

m	=	1000 (kg)	D	=	0.30 (m)
$-X_{\dot{u}}$	=	$0.05m$ (kg)	ρ	=	1025 (kg/m^3)
$-X_u$	=	$\frac{m-X_{\dot{u}}}{5.0}$ (kg/s)	w	=	0.2
$-X_{u\|u\|}$	=	$\frac{1}{2}\rho C_d A_{surge}$ (kg(m)	t	=	0.1
d_f	=	$\frac{-X_{u\|u\|}}{(1-t)w^2}$(kg/s)	J_m	=	1.0 (kgm^2)
d_0	=	$\frac{-X_u}{(1-t)w}$ (kg/m)	C_d	=	1.0
m_f	=	$\rho A l \gamma$ (kg)	A_{surge}	=	1.0 (m^2)
l	=	0.30 (m)	γ	=	1.0
A_{thruster}	=	$\pi\left(\frac{D}{2}\right)^2$ (m^2)			

Table 1: Model parameters.

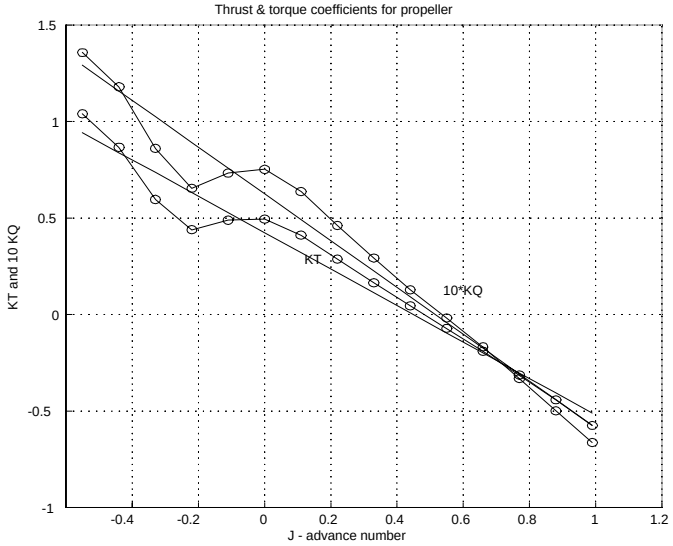

Figure 4: Experimental results for K_T and $10K_Q$ versus J_0 (circles) and least-squares fits to a straight line (solid lines).

8.2 Discussion of Simulation Results

The control laws were simulated by commanding a reference thrust of $T_d = 100$ (N) which was shifted to $T_d = -100$ (N) at $t = 30$ (sec), see Figure 6. The results form the simulation study can be summarized according to:

Estimation of Advance Speed Figure 5 shows the performance of the *nonlinear observer* is shown. Both estimation errors $\tilde{V}_a = V_a - \hat{V}_a$ and $\tilde{u} = u - \hat{u}$ (upper plots) are zero mean white noise processes. Even though the surge measurement u and shaft speed measurement n are corrupted with white noise with amplitudes 0.1 (m/s) and 0.1 (rps), and standard deviations of $\sigma = 0.0335$ in the simulation study, excellent convergence of $\hat{V}_a \to V_a$ is obtained (lower left plot). The estimate $\hat{V}_a$ is, however, more noisy than its true value V_a. This can be further improved by tuning of the observer gains. In addition, we see that we obtain good filtering of the noisy signal u (lower right plot).

Thrust Tracking Capabilities From Figure 6 it is seen that the *output feedback integral controller* has excellent thrust tracking capabilities (lower plots) while an offset in thrust is observed for the *PI-controller* (upper plots). The desired thrust $T_d = \pm 100$ (N) is transformed to shaft speed reference signals $\dot{n}_d$ and n_d by using (76)–(77). The offset in thrust for the PI-controller is due to variations in

shaft speed V_a. This is seen by plotting the components:

$$T_0 = T_{n|n|} n\,|n|\,, \qquad Q_0 = Q_{n|n|} n\,|n| \tag{111}$$

$$T_1 = -T_{|n|V_a}\,|n|\,V_a, \quad Q_1 = -Q_{|n|V_a}\,|n|\,V_a \tag{112}$$

together with the total thrust $T = T_0 + T_1$ and torque $Q = Q_0 + Q_1$. The PI-controller tracks $T = T_0 = T_d$ (the term T_1 is not available since V_a is unknown when using a PI-controller) while the nonlinear output feedback integral controller uses the estimate $\hat{V}_a$ to track the total thrust $T = T_0 + T_1 = T_d$. Another benefit of using the nonlinear observer in conjunction with an output feedback integral controller is that the estimate $\hat{V}_a$ can be used to compute a more accurate shaft speed reference n_d from T_d. This is seen from (76) where V_a is needed.

RPM Tracking Capabilities and Motor Torque Commands Figure 7 shows the shaft speed tracking performance for the two controllers and the corresponding motor torque commands (control inputs). Since the PI-controller does not use model information a high gain is needed in order to obtain good RPM tracking capabilities. This results in more noisy motor torque control signals then for the model-based nonlinear output feedback integral controller. It is also seen that the tracking performance for the nonlinear controller is better than the PI-controller mainly due to compensation of advance speed effects.

9 Conclusions

A high performance nonlinear output feedback integral controller for propeller shaft speed was presented in this paper. The control law was designed by first designing a nonlinear observer for the propeller axial flow (advance speed) and next using observer backstepping to produce a globally exponentially stable controller. The control law was also modified to include integral action resulting in a uniformly globally asymptotically and uniformly locally exponentially stable integral controller. The proposed output feedback controller was shown to be robust for disturbances in propeller revolution and torque.

The case study was an unmanned underwater vehicle propulsed with a single main propeller. The propeller was assumed driven by a DC motor and a simulation study was used to demonstrate the tracking capabilities of the observer and controller. The observer was capable of producing accurate estimates of the advance speed. Hence, this estimate could be used to compensate the effect of advance speed on the propeller thrust and torque. The estimate of the advance speed could also be used to compute more accurate set-points for the vehicle speed controller since the thrust commands could be more accurately mapped to propeller revolution commands.

Acknowledgments

The authors are grateful to Professors Knut Minsaas and Asgeir J. Sørensen at the Department of Marine Hydrodynamics, the Norwegian University of Science and Technology (NTNU) for useful discussions on steady and unsteady flow effects for propellers.

Parts of this work were performed while the first author visited the Department of Automatic Control, Aalborg University, Denmark in the period January-March 1999. The same author is grateful to the Department of Automatic Control, Aalborg University and the Norwegian Research Council for financial support in this period.

Appendix A: DC-Motor Dynamics

Consider a DC-motor (Fossen [8]):

$$L_a \frac{d}{dt} i_m = -R_a i_m - K_m \omega_m + V_m \tag{113}$$

$$J_m \dot{\omega}_m = K_m i_m - Q \tag{114}$$

where V_m is the armature voltage, i_m is the armature current, ω_m is the propeller revolution and Q is the load from the propeller. In addition, L_a is the armature inductance, R_a is the armature resistance, K_m is the motor torque constant and J_m is the rotor moment of inertia. Let n denote the propeller shaft speed in revolutions per second. Hence:

$$\omega_m = 2\pi n \tag{115}$$

Since the electrical time constant $T_a = L_a/R_a$ is small compared to the mechanical time constant, time scale separation suggests:

$$\frac{L_a}{R_a}\frac{d}{dt}i_m \approx 0 \tag{116}$$

Hence, the shaft speed dynamics is given by:

$$\begin{aligned} 0 &= -R_a i_m - 2\pi K_m n + V_m & (117)\\ 2\pi J_m \dot{n} &= K_m i_m - Q & (118) \end{aligned}$$

Motor Current Control

The motor current can be controlled by using a P-controller:

$$V_m = K_p(i_d - i_m), \quad K_p > 0 \tag{119}$$

where i_d is the desired motor current. From (117) we get:

$$(R_a + K_p)i_m = -2\pi K_m n + K_p i_d \tag{120}$$

The motor dynamics (118) for the current controlled motor therefore takes the form:

$$2\pi J_m \dot{n} + \frac{2\pi K_m^2}{R_a + K_p} n = \frac{K_m K_p}{R_a + K_p} i_d - Q \tag{121}$$

If a high gain controller $K_p \gg R_a > 0$ is used, this expression simplifies to:

$$2\pi J_m \dot{n} = K_m i_d - Q \tag{122}$$

Motor Torque Control

For a DC motor the motor torque will be proportional with the motor current. Hence, the desired motor torque Q_d can be written as:

$$Q_d = K_m i_d \tag{123}$$

From (121) we see that this yields the following dynamics for a torque controlled motor:

$$2\pi J_m \dot{n} + \frac{2\pi K_m^2}{R_a + K_p} n = \frac{K_p}{R_a + K_p} Q_d - Q \tag{124}$$

which reduces to

$$2\pi J_m \dot{n} = Q_d - Q \tag{125}$$

for $K_p \gg R_a > 0$.

Motor Voltage Control

Motor voltage control is obtained by combining (117)–(118) to yield:

$$2\pi J_m \dot{n} + \frac{2\pi K_m^2}{R_a} n = \frac{K_m}{R_a} V_m - Q \tag{126}$$

Unified DC-Motor Control Model

Based on the three models presented above, a unified control model for the DC-motor shaft speed dynamics can be written:

$$2\pi J_m \dot{n} + K_n n = \tau - Q \tag{127}$$

where motor *voltage*, *current* and *torque* control are obtained by choosing the control input τ and linear damping coefficient K_n according to Table 2:

	control input τ	Linear damping K_n
Voltage	$\frac{K_m}{R_a} V_m$	$\frac{2\pi K_m^2}{R_a}$
Current	$\frac{K_m K_p}{R_a + K_p} i_d$	$\frac{2\pi K_m^2}{R_a + K_p}$
Torque	$\frac{K_p}{R_a + K_p} Q_d$	$\frac{2\pi K_m^2}{R_a + K_p}$

Table 2: DC-motor control model.

References

[1] M. Blanke. Ship Propulsion Losses Related to Automated Steering and Prime Mover Control, *The Technical University of Denmark, Lyngby, Ph. D. dissertation*, 1981

[2] M. Blanke, R. Izadi-Zamanabadi and T. F. Lootsma. Fault Monitoring and Reconfigurable Control for a Ship Propulsion Plant. *Journal of Adaptive Control and Signal Processing, Vol. 12, pp. 671–688, December 1998.*

[3] J. P. Breslin and P. Andersen. *Hydrodynamics of Ship Propellers.* Cambridge University Press, UK, 1994.

[4] J. S. Carlton. *Marine Propellers and Propulsion.* Oxford: Butterworth-Heinemann, 1994.

[5] S. E. Cody. An Experimental Study of the Response of Small Thrusters to Step and Triangular Wave Inputs, *MSME thesis, Naval Postgraduate School, Monterey, CA*, 1992.

[6] O. M. Faltinsen. *Sea Loads and Offshore Structures.* Cambridge University Press, UK, 1990.

[7] O. M. Faltinsen and B. Sortland. Slow Drift Eddy Making Damping of a Ship. *Applied Ocean Research,* **AOR-9**(1):37–46.

[8] T. I. Fossen. *Guidance and Control of Ocean Vehicles,* John Wiley & Sons Ltd., 1994.

[9] T. I. Fossen and J. P. Strand. Passive Nonlinear Observer Design for Ships Using Lyapunov Methods: Full-Scale Experiments With a Supply Vessel. *Automatica.* **AUT-35**(1)3–16, 1999.

[10] A. J. Healey, S. M Rock, S. Cody, D. Miles and J. P. Brown. Toward an Improved Understanding of Thruster Dynamics for Underwater Vehicles, *IEEE Journal of Oceanic Engineering,* **JOE-29**(4):354–361, 1995.

[11] H. Khalil. *Nonlinear Systems.* McMillan Publishing Co., 2nd. Edition, New York, 1996.

[12] M. Krstic, I. Kanellakopoulos and P. Kokotovic. *Nonlinear and Adaptive Control Design.* John Wiley & Sons Ltd.

[13] E. V. Lewis (Ed.). *Principles of Naval Architecture,* SNAME, 1988.

[14] P. C. Lewis. Differential Equations Referred to a Variable Metric. *American Journal of Mathematics,* **AJM**-73:48-58, 1951.

[15] A. Loria, T. I. Fossen and A. Teel. UGAS and ULES of Non-Autonomous Systems: Applications to Integral Control of Ships and Robot Manipulators, *Proc. of the European Control Conference (ECC'99)*, Karlsruhe, Germany, August 1999.

[16] M. B. McLean. Dynamic Performance of Small Diameter Tunnel Thrusters, *MSME thesis, Naval Postgraduate School, Monterey, CA,* 1991.

[17] W. S. Lohmiller. Contraction Analysis of Nonlinear Systems. *Ph.D. Dissertation, Department of Mechanical Engineering, MIT*, MA, February 1999.

[18] W. Lohmiller and J.-J. Slotine. On Metric Controllers and Observers for Nonlinear Systems. *Proc. of the 35th Conf. on Decision and Control,* Kobe, Japan, pp. 1477–1482, December 1996.

[19] W. Lohmiller and J.-J. Slotine. On Contraction Analysis for Nonlinear Systems, *Automatica* **AUT-6**, 1998.

[20] J. N. Newman *Marine Hydrodynamics.* MIT Press, Cambridge, Massachusetts, 1977.

[21] H. Nijmeijer and T. I. Fossen (Eds.). *New Directions in Nonlinear Observer Design.* Springer-Verlag London Ltd., 1999.

[22] M. W. C. Oosterveld and P. van Oossanen. Further Computer-Analyzed Data of the Wageningen B-Screw Series. *Int. Shipbuilding Progress,* **ISP-22**:251-262, 1975.

[23] A. J. Sørensen, A. K. Ådnanes, T. I. Fossen and J. P. Strand. A New Method of Thruster Control in Positioning of Ships Based on Power Control, *Proc. of the 4th IFAC Conference on Manoeuvering and Control of Marine Craft, 10-12 September, 1997, Brijuni, Croatia.*

[24] C. L. Tsukamoto, W. Lee, J. Yuh, K. Choi and J. Lorentz. Comparison Study on Advanced Thruster Control of Underwater Robots. *Proc. of the Int. Conf. on Robotics and Automation,* Albuquerque, New Mexico, pp. 1845-1850, April 1997.

[25] L. L. Whitcomb and D. R. Yoerger. Comparative Experiments in the Dynamics and Model-Based Control of Marine Thrusters. *Proc. of the IEEE/MTS Oceans'95, Vol. 2, pp. 1019–1028, 1995.*

[26] L. L. Whitcomb and D. Yoerger. Development, Comparison, and Preliminary Experimental Validation of Nonlinear Dynamic Thruster Models. *IEEE Journal of Oceanic Engineering, 1999,* to appear.

[27] L. L. Whitcomb and D. Yoerger. Preliminary Experiments in Model Based Thruster Control for Underwater Vehicle Position Control. *IEEE Journal of Oceanic Engineering, 1999,* to appear.

[28] D. R. Yoerger, J. G. Cooke and J.- J. E. Slotine. The Influence of Thruster Dynamics on Underwater Vehicle Behavior and their Incorporation into Control System Design, *IEEE Journal of Oceanic Engineering*, **JOE-15**(3):167–178, 1991.

[29] W. W. Zhou and M. Blanke. Identification of a Class of Nonlinear State-Space Models Using RPE Techniques. *IEEE Trans. on Automatic Control,* **TAC-34**(3):312–316, 1989.

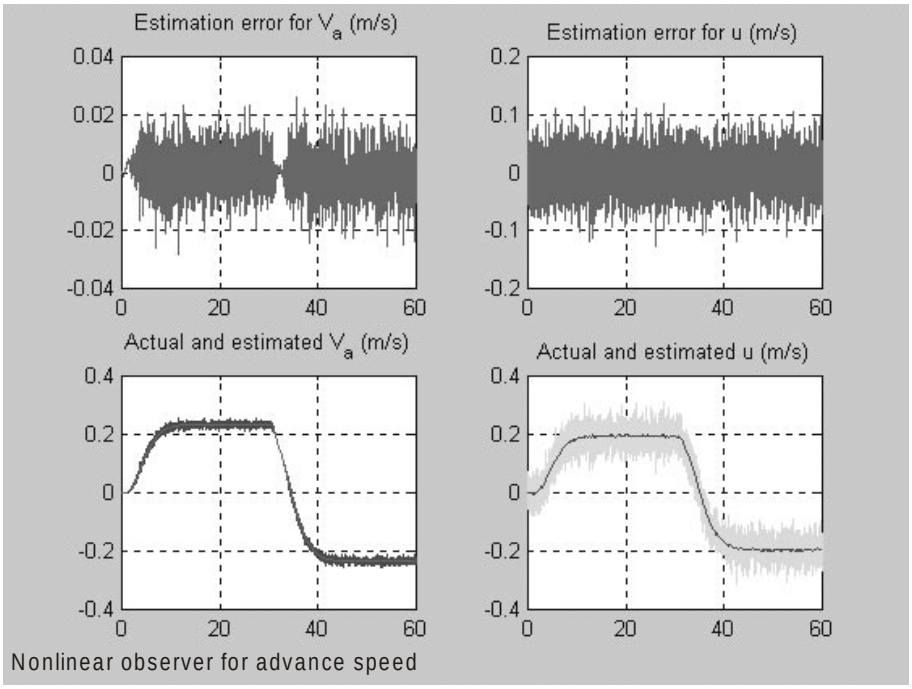

Figure 5: Upper plots: estimation errors $\tilde{V}_a$ and $\tilde{u}$ versus time. Lower plots: actual advance speed V_a and measured surge speed u together with their estimates $\hat{V}_a$ and $\hat{u}$ versus time.

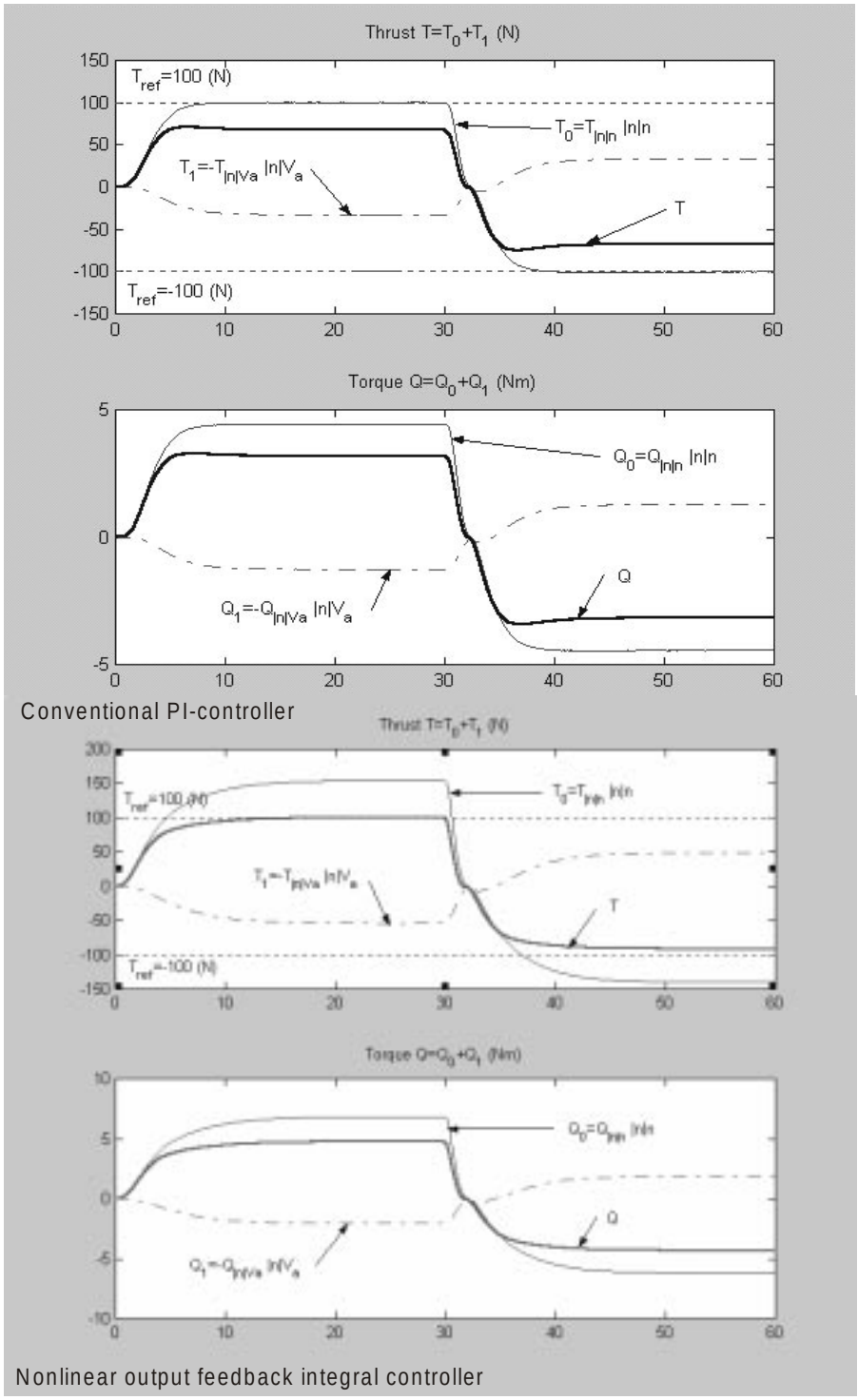

Figure 6: Thrust T and torque Q for plots for a conventional PD-controller (upper plots) and the nonlinear output feedback controller (lower plots) versus time. Notice the offset in thrust for the PD-controller (no compensation of advance speed).

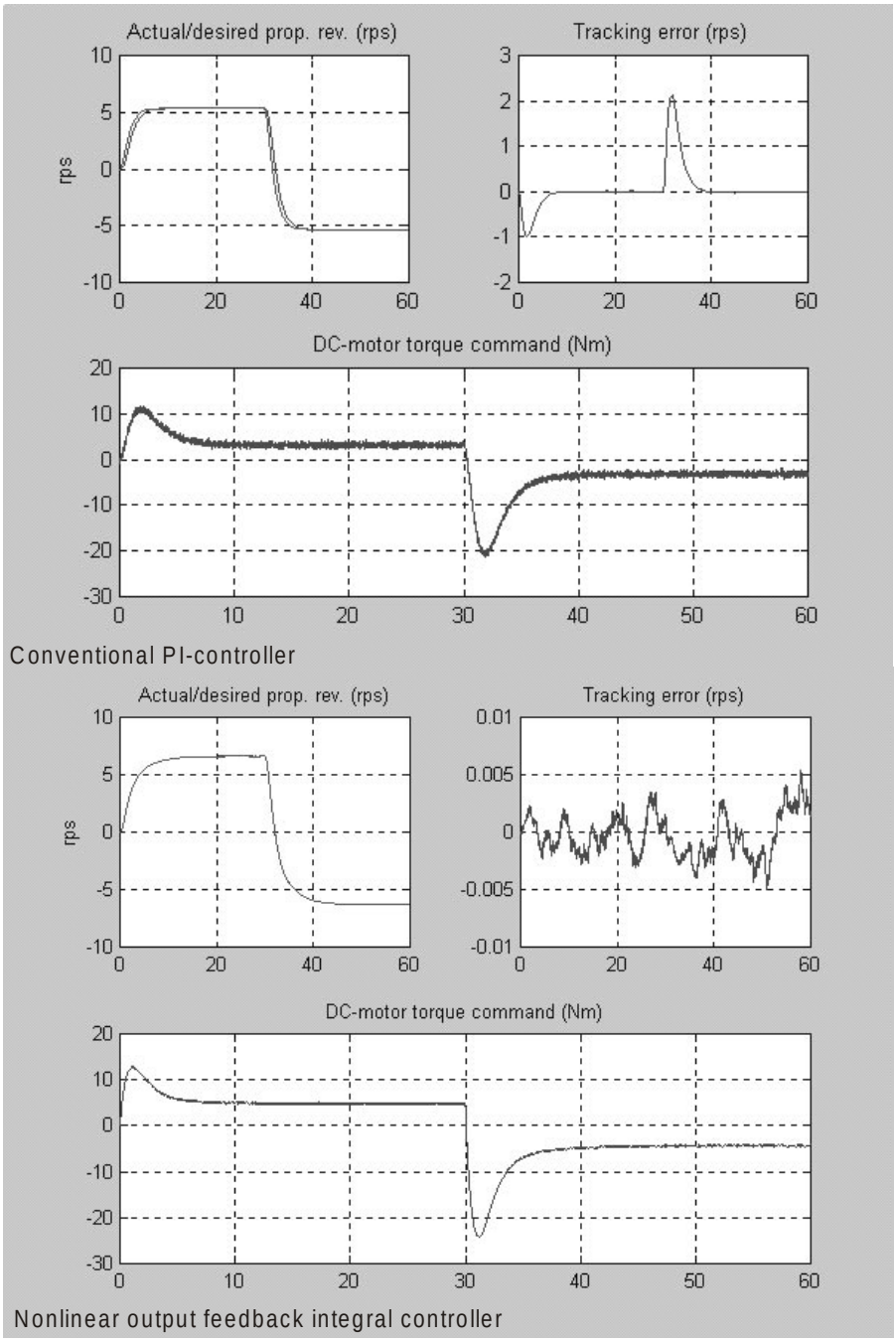

Figure 7: Actual, n, and desired, n_d, propeller revolutions, tracking errors, $n - n_d$, and motor torque, Q_d, commands for a conventional PD-controller (upper plots) and the nonlinear output feedback controller (lower plots) versus time.